Journal of Chromatography A, 1217 (2010) 7109–7122

Contents lists available at ScienceDirect

Journal of Chromatography A

journal homepage: www.elsevier.com/locate/chroma

Characterization and identification of steroidal alkaloids in *Fritillaria* species using liquid chromatography coupled with electrospray ionization quadrupole time-of-flight tandem mass spectrometry

Jian-Liang Zhou [1], Gui-Zhong Xin [1], Zi-Qi Shi, Mei-Ting Ren, Lian-Wen Qi, Hui-Jun Li, Ping Li *

Key Laboratory of Modern Chinese Medicines (China Pharmaceutical University), Ministry of Education, Nanjing 210009, China

ARTICLE INFO

Article history:
Received 31 March 2010
Received in revised form 16 August 2010
Accepted 7 September 2010
Available online 16 September 2010

Keywords:
LC/ESI-QTOF-MS/MS
Fritillaria
Steroidal alkaloids
Characterization
Fragmentation

ABSTRACT

Liquid chromatography coupled with electrospray ionization quadrupole time-of-flight tandem mass spectrometry (LC/ESI-QTOF-MS/MS) was performed to study the fragmentation behaviors of steroidal alkaloids from *Fritillaria* species, the antitussive and expectorant herbs widely used in traditional Chinese medicine. We propose, herein, a strategy that combining key diagnostic fragment ions and the relative abundances and amounts of major fragment ions (the ions exceeding 10% in abundance) to distinguish different sub-classes of *Fritillaria* alkaloids (FAs). It was found that hydrogen rearrangement and induction effects result in ring cleavage of the basic skeletons occurred in the MS/MS process and produced characteristic fragment ions, which are useful for structural elucidation. This method was finally used to investigate the primary steroidal alkaloids in the extracts of eight major *Fritillaria* species. As a result, 41 steroidal alkaloids (29 cevanine type, 1 jervine type, 6 veratramine type and 5 secosolanidine type alkaloids) were selectively identified in these *Fritillaria* species. Twenty-six compounds were unambiguously identified by comparing with the reference compounds and 15 compounds were tentatively identified or deduced according to their MS/MS data. Logical fragmentation pathways for different types of FAs have been proposed and are useful for the identification of these types of steroidal alkaloids in natural products especially when there are no reference compounds available.

1. Introduction

Fritillaria, a genus of perennial herbs, is widely distributed in Mediterranean Region, North America and Central Asia. Many species of *Fritillaria* were traditionally used as herbal remedies in Japanese, Turkish, Pakistani and south-east Asian folk medicines [1–3], while bulbs of many *Fritillaria* species growing in China have been used as antitussive and expectorant herbs using the Chinese name "Beimu" in traditional Chinese medicine (TCM) for thousands of years [4]. Based on various chemical and pharmacological studies, steroidal alkaloids from *Fritillaria* species (*Fritillaria* alkaloids, FAs), which including verticine, verticinone, peimisine, ebeiedine, ebeiedinone, hupehenine, imperialine, puqietinone etc., have been demonstrated as the major bioactive ingredients in "Beimu" [5–11]. And they commonly possess various biological activities, such as antihypertensive [5,6], anticholinergic [7–9], antitumour [10], anti-asthmatic and antitussive activities [10,11].

FAs display the characteristic steroidal framework, which processing a C27 cholestane carbon skeleton with five or six carbocyclic or heterocyclic rings. Based on the basic structural skeleton, FAs can be divided into several sub-classes, such as cevanine, jervine, veratramine and secosolanidine types [12]. A wide range of structural variation is observed in the *Fritillaria* species, which differs in terms of the number, position, and nature of the functional groups. Therefore, improvements in structural characterization of FAs, particularly from complex matrices, would facilitate the understanding of their chemical and biological properties.

Generally, the structural analysis of FAs is performed by a combination of chromatographic and spectroscopic methods, including gas chromatography (GC), liquid chromatography-ultraviolet (LC-UV), LC-evaporative light scattering detection (ELSD), nuclear magnetic resonance (NMR), and LC–mass spectrometry (MS). However, owing to the characteristic structure of FAs lacking of volatility and useful chromophores, GC and LC-UV methods are not the first choice for analysis of FAs. Moreover, low sensitivity and possible uncertainty of chromatographic peak identification (mainly by comparing retention time with reference compounds) made LC-UV and -ELSD methods unlikely match the structural elucidation

* Corresponding author at: Department of Pharmacognosy, Key Laboratory of Modern Chinese Medicines (China Pharmaceutical University), Ministry of Education, No.24, Tongjia Lane, Nanjing 210009, China. Tel.: +86 25 8327 1379; fax: +86 25 8327 1379.
E-mail addresses: liping2004@126.com, fleude@126.com (P. Li).
[1] These authors contributed equally to this work.

0021-9673/$ – see front matter © 2010 Elsevier B.V. All rights reserved.
doi:10.1016/j.chroma.2010.09.019

of FAs [13]. Although NMR is the most efficient method for structural elucidation of chemical compounds, a relatively large amount of purified sample is required and the isolation procedure from a complicated mixture is very time-consuming and costly. Among these techniques, LC–MS, especially when coupled to a soft ionization source e.g. electrospray ionization (ESI), has become a very powerful tool in the analysis of FAs. The coupling of LC and ESI-MS combines the efficient separation capability of LC and the great power of structural characterization of MS [14]. Recently, LC/ion trap multistage mass spectrometry (IT-MS^n) and/or LC/triple-quadrupole MS have been successfully applied to the identification and characterization of natural compounds [14,15]. For example, Li et al. have reported on detailed studies of the fragmentation behaviors of 17 steroidal alkaloids from the Chinese herb *Veratrum nigrum* L. (*Veratrum* alkaloids) by LC–ESI-IT-MS^n [16]. Nevertheless, in most studies using low-resolution MS instruments, such as IT-MS and triple-quadrupole MS, it is difficult to confirm the identities of the product ions. Whereas, high-resolution time-of-flight mass spectrometry (TOF-MS) constitutes a higher order mass identification than those afforded by nominal mass measurements obtained by other types of mass analyzers, such as triple-quadrupole MS and IT-MS [17–19]. This property of TOF-MS makes it an attractive analytical technique to perform structure elucidation or confirmation from complex matrices. When coupled to a quadrupole mass filter, QTOF-MS/MS permits fragmentations analysis with accurate mass measurements for both precursor and product ions, which facilitates the elucidation of characteristic fragmentation pathways of target or non-target compounds.

In our previously study, we reported a LC/TOF-MS method for determination of steroidal alkaloids in *Fritillaria* species, but we could not obtain available fragment ions to perform the structure identification of FAs, especially for the non-target FAs [13]. Therefore, the aim of this study is to show the potential of LC/QTOF-MS/MS for structure elucidation of steroidal alkaloids in *Fritillaria* species for complementing the blank on the topic of systematic characterization and fragmentation mechanism study of FAs. Firstly, in this work, fragmentation rules and key diagnostic fragment ions for the 26 reference compounds of FAs have been summarized, and possible pathways of fragmentation have been proposed. Based on the fragmentation behavior of these reference compounds, LC/ESI-QTOF-MS/MS was then used to characterize the FAs in eight different *Fritillaria* species.

2. Experimental

2.1. Chemicals and reagents

Acetonitrile (ACN) and methanol are of HPLC grade from Merck (Darmstadt, Germany), ammonium formate of analytical grade was purchased from Shanghai Lingfeng Chemical Reagent Co., Ltd. (Shanghai, China) and formic acid with a purity of 96% is of HPLC grade (Tedia, USA). Deionized water (18 MΩ) was prepared by distilled water through a Milli-Q system (Millipore, Milford, MA, USA). Other reagents were of analytical purity.

The steroidal alkaloid reference compounds, puqienine F (**P2**), imperialine-3-β-D-glucoside (**P4**), puqienine C (**P5**), puqienine D (**P9**), imperialine (**P10**), peimisine (**P12**), verticine N-oxide (**P13**), puqienine E (**P14**), puqiedine-7-ol (**P15**), hupeheninoside (**P16**), puqietinonoside (**P17**), verticine (**P18**), verticinone N-oxide (**P19**), yibeinoside A (**P21**), verticinone (**P22**), puqienine B (**P23**), puqienine A (**P25**), isoverticine (**P31**), puqietinone (**P33**), ebeiedinone (**P34**), N-demethylpuqietinone (**P35**), puqiedinone (**P37**), ebeienine (**P38**), ebeiedine (**P39**), puqiedine (**P40**), and puqietinedinone (**P41**) (Fig. 1), were isolated from several *Fritillaria* species in our laboratory [10,20,21–24], and their identities were confirmed by IR, ^{1}H- and ^{13}C-NMR, MS analyses. The purity of these steroidal alkaloids was determined to be more than 98% by normalization of the peak areas detected by HPLC with ESI/MS. Stock standard solutions of 26 reference steroidal alkaloids were prepared in methanol at a final concentration of 40 μg/ml. These solutions were stored at 4 °C for further study.

2.2. Sample preparation

A total of eight *Fritillaria* species (including *F. thunbergii* (**A**), *F. ebeiensis* (**B**), *F. hupehensis* (**C**), *F. pallidiflora* (**D**), *F. walujewii* (**E**), *F. cirrhosa* (**F**), *F. ussuriensis* (**G**), and *F. puqiensis* (**H**)) were collected from various areas of China and authenticated by Professor Ping Li. The voucher specimens were deposited at the Herbarium of China Pharmaceutical University, Nanjing, China.

The dried bulbs of *Fritillaria* species were powdered to a homogeneous size, and sieved through a No. 60 mesh, followed by drying at 60 °C in the oven for 2 h. The dried bulb powders (200–500 mg, adjusted according to the alkaloid contents of each *Fritillaria* species) were pre-alkalized with 2 ml ammonia solution (25%) for 1 h, and immersed in 25 ml trichlormethane:methanol (4:1, v/v) mixture overnight, then ultrasonicated for 2 h. After being filtered, the extracts (10 ml) were concentrated to dryness in vacuum at 50 °C. The residue was made up to exactly 2 ml with initial mobile phase using a volumetric flask. The resultant solutions were centrifuged at 12,000 rpm for 10 min; the supernatants were transferred to an autosampler vial for LC/QTOF-MS/MS analysis.

2.3. Liquid chromatography

Chromatographic analysis was performed on an Agilent 1200 Series (Agilent Technologies, Germany) LC system equipped with a binary pump, an online degasser, an auto plate-sampler, and a thermostatically controlled column compartment. Chromatographic separation was carried out at 25 °C on an Agilent ZorBax Extend-C_{18} column (4.6 mm × 250 mm, 5 μm). The mobile phase consisted of water (10 mM ammonium formate) with 0.1% formic acid (A) and acetonitrile (B) using a gradient elution of 15–25% B at 0–10 min, 25–30% B at 10–32 min, 30–50% B at 32–37 min, 50–60% B at 37–42 min, 60–100% B at 42–43 min. A 10-min post run time back to the initial mobile phase composition was used after each analysis. The flow rate was kept at 0.8 ml/min, and was split at the column outlet to allow 50% eluent to flow into the mass spectrometer. The sample volume injected was set at 2 μL.

2.4. Mass spectrometry

Mass spectrometry was performed using an Agilent 6530 QTOF MS (Agilent Corp, USA) equipped with an electrospray ionization (ESI) interface, and using the following operating parameters: drying gas (N_2) flow rate, 5.0 l/min; drying gas temperature, 325 °C; nebulizer, 45 psig; sheath gas temperature, 400 °C; sheath gas flow, 10 l/min; capillary, 3500 V; skimmer, 65 V; OCT 1 RF Vpp, 750 V; fragmentor voltage, 100 V. The sample collision energy was set at 50 and 70 V. All the operations, acquisition, and analysis of data were controlled by Agilent LC–MS-QTOF MassHunter Acquisition Software Ver. A.01.00 (Agilent Technologies) and operated under MassHunter Workstation Software Version B.02.00 (Agilent Technologies). Each sample was analyzed in positive mode to provide information for structural identification. Mass spectra were recorded across the range *m*/*z* 100–1000 with accurate mass measurement of all mass peaks. The $[M+H]^+$ ions of FAs were used as the precursor ions to obtain the product ions for structure identification of FAs in different samples.

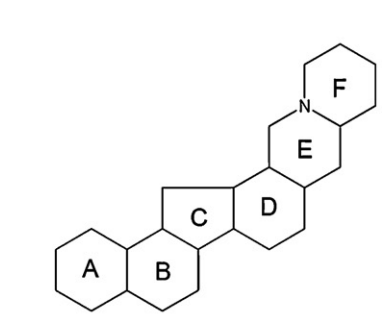

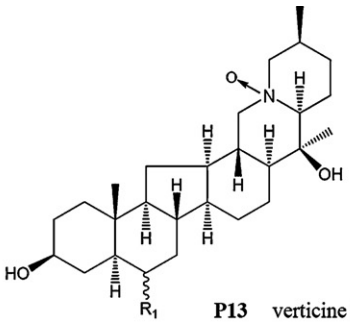

		R_1
P13	verticine N-oxide	α-OH
P19	verticinone N-oxide	=O

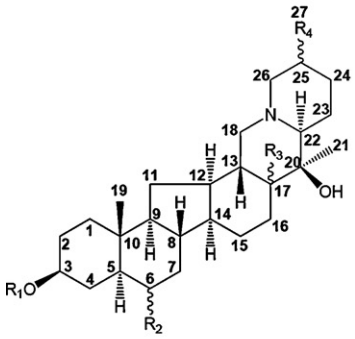

		R_1	R_2	R_3	R_4
P18	verticine	H	α-OH	α-H	β-Me
P22	verticinone	H	=O	α-H	β-Me
P31	isoverticine	H	β-OH	α-H	β-Me
P10	imperialine	H	=O	β-H	β-Me
P4	imperialine-3-β-D-glucoside	Glc	=O	β-H	β-Me
P8	zhebeinone-3-β-D-glucoside or verticinone-3-β-D-glucoside	Glc	=O	α-H	α-Me
		Glc	=O	α-H	β-Me
P7	zhebeininoside	Glc	α-OH	α-H	α-Me

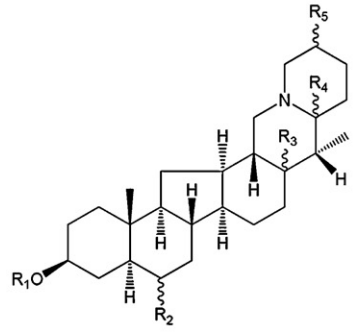

		R_1	R_2	R_3	R_4	R_5
P39	ebeiedine	H	β-OH	α-H	α-H	β-Me
P34	ebeiedinone	H	=O	α-H	α-H	β-Me
P40	puqiedine	H	β-OH	α-H	α-H	α-Me
P37	puqiedinone	H	=O	α-H	α-H	α-Me
P21	yibeinoside A	Glc	=O	β-H	α-H	β-Me
P16	hupeheninoside	Glc	β-OH	β-H	α-H	β-Me
P28	ebeiedine-3-β-D-glucoside	Glc	β-OH	α-H	α-H	β-Me
P29	hupehenine	H	β-OH	β-H	α-H	β-Me
P24	yibeinoside B	Glc	=O	β-H	β-Me	β-Me
P32	sinpeinine A	H	=O	β-H	α-H	β-Me

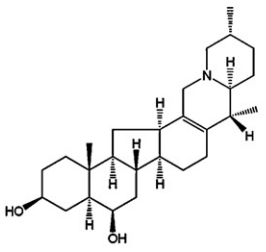

P38 ebeienine

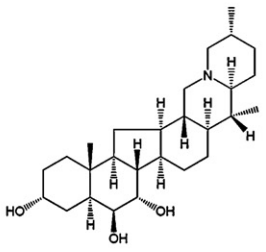

P15 puqiedine-7-ol

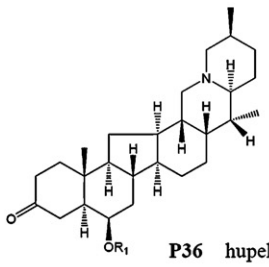

		R_1
P36	hupehenirine	H
P27	yubeiside	Glc

Fig. 1. Chemical structures of steroidal alkaloids identified in the extracts of eight *Fritillaria* species.

3. Results and discussion

3.1. Optimization of HPLC conditions and the MS collision energy

In order to develop and validate a highly sensitive and selective method, the chromatographic conditions, especially the composition of mobile phase and the type of column, were optimized through several trials to achieve the desired separation, run time and symmetric peak shapes for the constituents. In our previously LC/TOF-MS method, we successfully separated FAs by using basic mobile phase, but the analytical time was more than 90 min [13]. As reported [25], basic or high-salt mobile phases are not bene-

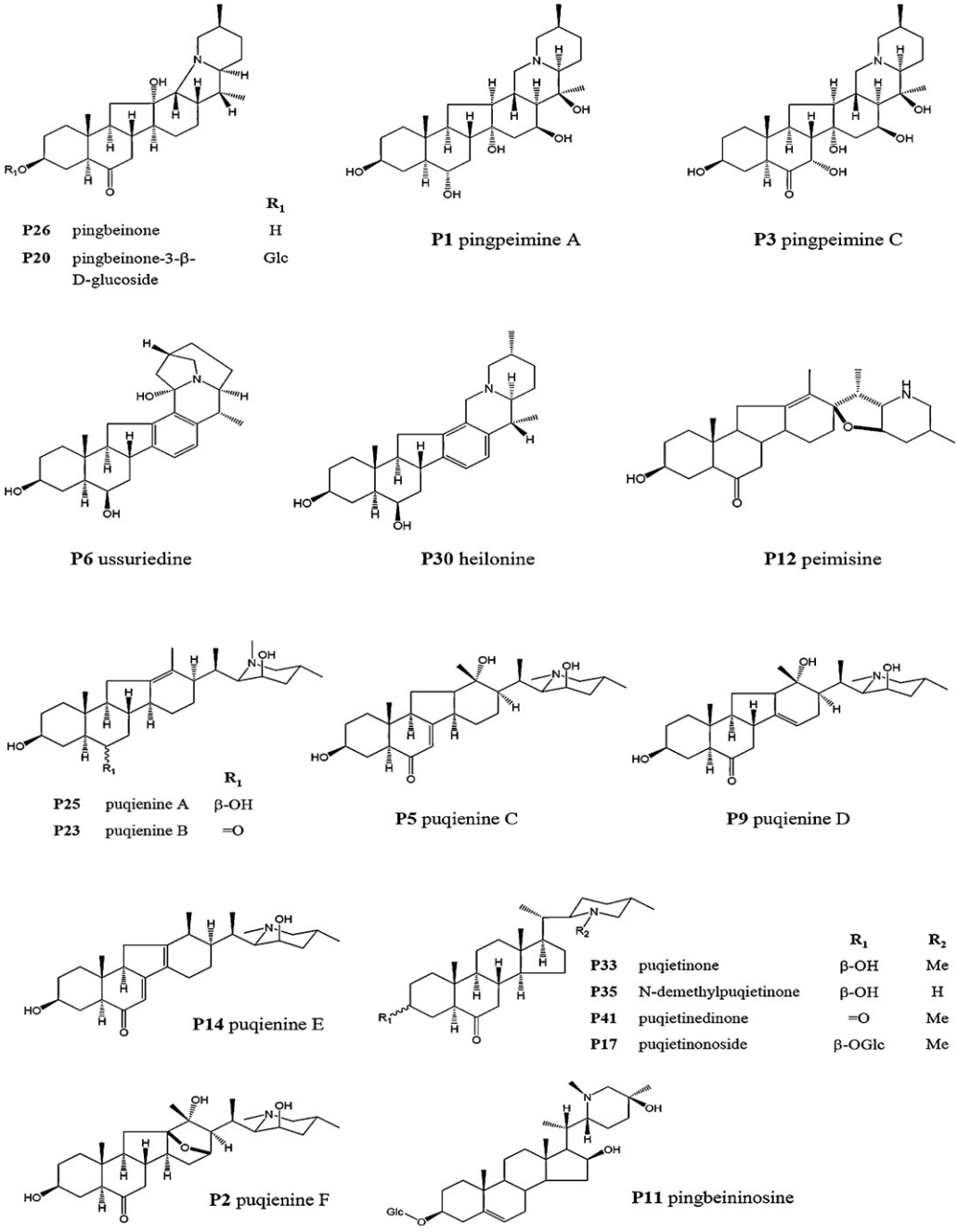

Fig. 1. (*Continued*).

ficial for the ionization of basic compounds, which decrease the ESI^+ sensitivity compared with acidic mobile phases. In this paper, thus, the acidic mobile phase consisting of acetonitrile and water containing 0.1% formic acid was firstly selected and various linear gradients of acetonitrile and aqueous solution at a flow rate of 0.8 ml/min were investigated to rapidly separate the 26 reference compounds of FAs on an Agilent ZorBax Extend-C_{18} column (4.6 mm × 250 mm, 5 μm). By the optimal gradient elution, most of the peaks could be separated within 40 min (see Supplementary material Figure S1A). Furthermore, to improve chromatographic behavior, reduce the peak tailing and facilitate ionization further, we optimized the composition of aqueous solution with ammonium formate and formic acid. We did comparative experiments by using 5 mM ammonium formate and 10 mM ammonium formate (both with 0.1% formic acid) as buffer aqueous solution, and the latter result in more improved chromatographic behavior and symmetric peak shapes (Figure S1B). Therefore, we selected the mobile phase consists of water (10 mM ammonium formate and 0.1% formic acid) and acetonitrile as the optimal composition of mobile phase to carry on the process of optimization of HPLC conditions. We also carried out the same trials using a fast HPLC column with sub-2 μm particle size (Agilent Zorbax StableBond-C_{18}, 4.6 mm × 50 mm, 1.8 μm) to reduce the run time. And the optimal conditions of the fast HPLC column trial were as following: use the mobile phase consists of water (10 mM ammonium formate and 0.1% formic acid) (A) and acetonitrile (B) to gradient elute at a flow rate of 0.35 ml/min. Unfortunately, the fast HPLC column was demonstrated to be not suitable for separating such more analytes

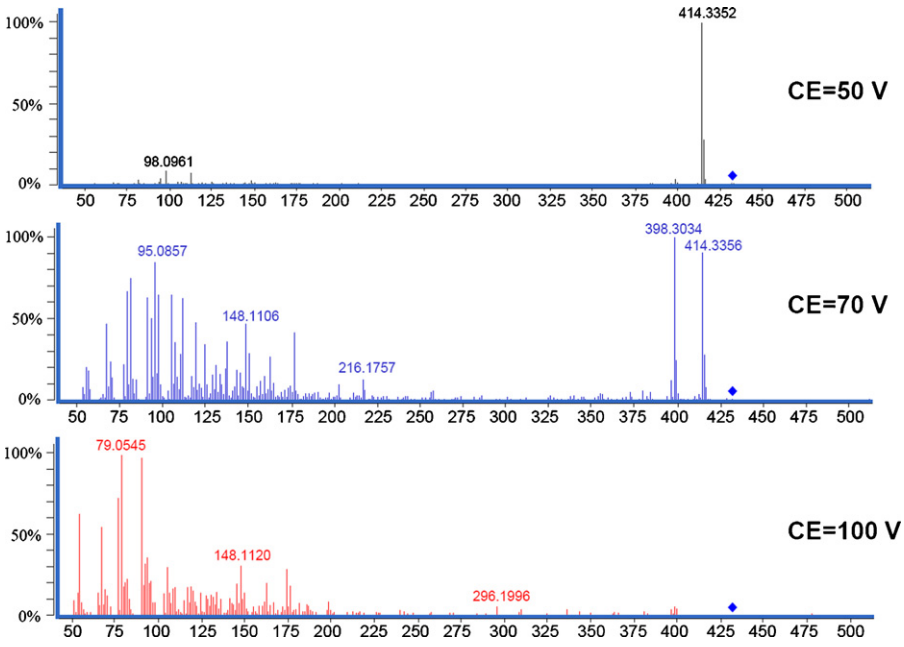

Fig. 2. MS/MS spectra for compound **P31** (isoverticine) at different collision energy.

due to the similar structure characteristic of these FAs (Figure S1C). Thus, the optimized chromatographic conditions are described in Section 2.3.

For the purpose of getting the optimized collision energy (CE) that generates available fragment information for structural elucidation and characterization, we performed MS/MS experiments at different CE. Taking compound **P31** (isoverticine) as an example, the optimization of MS collision energy are as follows. The parent ion (*m*/*z* 432.34, $[M+H]^+$) of **P31** was subjected to collisionally activated dissociation at different CE, and the resulting MS/MS spectra are shown in Fig. 2. When 50 V was used as the CE, the MS/MS spectra predominantly showed product ions formed by loss of substituent group. When the CE was increased to 70 V, the fragmentation spectra of the **P31** showed abundant product ions formed by loss of substituent group and cleavage of the rings of the basic skeleton. When the CE was increased to 100 V, the MS/MS spectra predominantly showed fragment ions resulted from cleavage of the rings of the basic skeleton. Even though the optimum CE might vary for different FAs, our study showed that 70 V CE is sufficient to cause abundant fragment ions for structure elucidation. In order to investigate the fragmentation behavior of FAs accurately, we proposed to combine the MS/MS spectra at 50 V and 70 V CE for characterization.

3.2. Characterization of the reference compounds

In the positive-ion ESI experiments, the CE was set at 50 V and 70 V to investigate the fragmentation behavior of the entire 26 reference compounds of FAs, respectively. Based on the basic structural skeleton, we grouped the 26 FAs into cevanine type (**P4**, **P10**, **P13**, **P15**, **P16**, **P18**, **P19**, **P21**, **P22**, **P31**, **P34**, **P37**, **P38**, **P39**, and **P40**), jervine type (**P12**), veratramine type (**P2**, **P5**, **P9**, **P14**, **P23**, and **P25**) and secosolanidine type (**P17**, **P33**, **P35**, and **P41**). According to whether there is hydroxy group in 20-position, the cevanine type can be classified into C20-OH substituent group (**P18**, **P22**, **P31**, **P4**, **P10**, **P13**, and **P19**) and No-C20-OH substituent group (**P15**, **P16**, **P21**, **P34**, **P37**, **P38**, **P39**, and **P40**). In the process of data analysis, we found that different types of FAs posses many similar fragment ions differing in relative abundance only, which result in significant difference in constituents of top five ions (in abundance ≥10%) of the four types of FAs. The ions with high intensity (in top 5) which commonly present in the identical type FAs were selected as the key diagnostic fragment ions. For some types of FAs, there are less than five ions with intensity higher than 10%, while for others, there are more than five ions exceeding 10% in abundance. Thus, the number of major fragment ions as well as their relative abundance can also be used as a diagnostic factor. Consequently, we propose, herein, a strategy combining key diagnostic fragment ions and the relative abundances and amounts of major fragment ions (the ions exceeding 10% in abundance) for identification of different FAs (see Table 1).

3.2.1. Cevanine type FAs

The cevanine type, structurally characterized by the hexacyclicbenzo [7,8] fluoreno [2,1] quinolizine nucleus, is the largest representative group of FAs. In ESI^+ mode, strong $[M+H-H_2O]^+$ ions were observed for most of the C20-OH substituent group alkaloids except for two *N*-oxides (**P13**, **P19**) at 50 V CE, which indicates that this group of alkaloids is easy to lost a molecule of water at a low CE. While for the No-C20-OH substituent group, $[M+H-H_2O]^+$ ions were replaced by $[M+H]^+$ as strong ions. The different structural feature between the two group is whether or not possessing of a hydroxyl at the 20-position which may be activated by the N atom in E-ring then is expelled as water. Except for the base peak ion, the two groups of cevanine type FAs yield similar fragment ions. Therefore, we take verticine (**P18**, a member of C20-OH substituent FAs) as the representative example to elucidate the fragmentation pathway of cevanine type FAs.

The ESI^+-MS/MS data and spectra for verticine are given in Table 1 and Fig. 3. In positive ion mode with the CE of 50 V, verticine produced a dominant $[M+H-H_2O]^+$ ion at *m*/*z* 414.33 ($C_{27}H_{44}NO_2$) and a minor protonated ion $[M+H]^+$ at *m*/*z* 432.34. With the CE increased to 70 V, it yields several characteristic fragment ions. Based on investigating these fragment ions, we summed up the possible fragmentation pathway of verticine displayed in Fig. 4(A–C). As we deduced, one of the probably protonated positions was the hydroxyl at 20-position (see Fig. 4A), which result in the protonated ion $[M+H]^+$ at *m*/*z* 432.34. When the CE increased to 70 V, several product ions, such as those at *m*/*z* 414.33, 138.12, 112.11, 398.30, and 176.14, were observed as characteristic fragments produced by

Table 1
Precursor and product ions of 26 reference compounds of FAs at different CE (the diagnostic ions were marked by underline).

Skeleton type	No.	t_R (min)	$[M+H]^+$	CE	Top five ions in abundance ≥10%	Other ions				
Cevanine type	**P18**	13.58	432.3463	50 V	414.3355 (100%)					398.3029, 138.1266, 124.1113, 112.1118, 98.0968, 95.0858, 81.0701, 67.0536, 55.0544
C20-OH				70 V	95.0855 (100%)	398.3029 (95.85%)	414.3345 (74.76%)	81.0700 (68.61%)	105.0693 (68.56%)	176.1441, 162.1268, 148.1108, 138.1272, 124.1116, 112.1119, 98.0960, 91.0539, 79.0543, 67.0546, 55.0546
	P22	15.24	430.3316	50 V	412.3202 (100%)					396.2872, 176.1429, 148.1125, 112.1116, 98.0965, 95.0843, 55.0546
				70 V	396.2891 (100%)	91.0544 (90.89%)	412.3211 (78.95%)	148.1108 (73.63%)	98.0963 (67.31%)	176.1436, 112.1114, 110.0957, 105.0707, 93.0691, 79.0547, 67.0548, 55.0547
	P31	19.60	432.3468	50 V	414.3352 (100%)					398.3018, 148.1109, 124.1116, 112.1113, 98.0961, 95.0853, 81.0688
				70 V	398.3034 (100%)	414.3356 (98.98%)	95.0857 (91.07%)	79.0546 (72.08%)	81.0696 (71.26%)	176.1435, 148.1106, 119.0851, 112.1117, 105.0701, 98.0966, 91.0543, 67.0548, 55.0544
	P4	8.93	592.3828	50 V	574.3703 (100%)	138.1268 (19.43%)				592.3855, 412.3175, 139.1302, 98.0963, 85.0291
				70 V	138.1274 (100%)	574.3717 (20.16)	96.0809 (10.51%)			412.3207, 394.3075, 139.1312, 112.1114, 98.0958, 79.0549, 69.0702, 55.0546
	P10	12.14	430.3317	50 V	138.1276 (100%)	412.3201 (67.47%)				396.2840, 139.1307, 112.1112, 98.0970, 96.0814, 69.0707, 55.0551
				70 V	138.1271 (100%)	96.0808 (39.91%)	69.0699 (13.18%)			412.3166, 396.2879, 139.1303, 79.0538, 67.0538, 55.0549
	P13	12.67	448.3420	50 V	112.1119 (100%)	448.3402 (13.85%)	98.0962 (12.09%)			430.3310, 412.3187, 386.3069, 138.1285, 96.0808, 82.0662, 69.0705
				70 V	112.1118 (100%)	98.0962 (19.75%)	96.0808 (16.55%)	69.0703 (15.21%)	55.0546 (10.48%)	412.3152, 95.0839, 82.0655, 67.0549
	P19	13.89	446.3271	50 V	112.1118 (100%)	98.0963 (14.87%)	446.3256 (10.37%)			428.3172, 410.3017, 384.2985, 138.1279, 96.0801, 82.0657, 69.0698, 58.0651
				70 V	112.1116 (100%)	98.0973 (16.96%)	69.0697 (15.23%)	96.0806 (15.15%)	55.0549 (11.24%)	138.1271
No-C20-OH	**P15**	12.88	432.3482	50 V	432.3460 (100%)					414.3362, 98.0963, 95.0857, 81.0691
				70 V	432.3463 (100%)	98.0965 (70.01%)	81.0700 (61.39%)	79.0542 (43.38%)	105.0694 (42.11%)	414.3333, 112.1122, 95.0856, 91.0536, 67.0545, 55.0554
	P34	25.13	414.3369	50 V	414.3360 (100%)					396.3273, 119.0851, 105.0687, 98.0964, 95.0861, 93.0706, 81.0713, 69.0711, 67.0552
				70 V	98.0955 (100%)	67.0544 (78.40%)	91.0547 (68.77%)	79.0546 (65.71%)	81.0697 (65.11%)	396.3265, 119.0851, 112.1113, 105.0703, 69.0703, 55.0542
	P37	27.40	414.3362	50 V	414.3357 (100%)					396.3258, 112.1112, 98.0973, 95.0854, 81.0710, 67.0550, 55.0549

Table 1 (*Continued*)

Skeleton type	No.	t_R (min)	$[M+H]^+$	CE	Top five ions in abundance ≥10%	Other ions				
				70 V	67.0540 (100%)	91.0546 (96.69%)	81.0696 (83.7%)	98.0963 (70.55%)	93.0694 (69.61%)	414.3343, 396.3236, 145.0983, 131.0842, 119.0844, 112.1118, 105.0690, 79.0548, 69.0697, 55.0540
	P39	28.83	416.3509	50 V	416.3510 (100%)					398.3400, 98.0965, 95.0849, 81.0701, 79.0537, 67.0548, 55.0552
				70 V	81.0700 (100%)	98.0962 (97.07%)	416.3521 (77.13%)	67.0542 (64.78%)	95.0861 (63.60%)	398.3407, 220.2047, 159.1146, 145.0998, 131.0855, 119.0854, 107.0858, 105.0696, 91.0541, 79.0545, 55.0555
	P40	33.98	416.3525	50 V	416.3509 (100%)					398.3389, 107.0851, 98.0957, 95.0869, 81.0700, 67.0542, 56.0489
				70 V	81.0696 (100%)	416.3518 (94.32%)	98.0962 (88.98%)	67.0547 (85.46%)	79.0541 (70.65%)	398.3361, 356.2913, 220.2028, 171.1131, 145.0985, 119.0854, 105.0692, 95.0850, 91.0538, 55.0546
	P16	13.18	578.4032	50 V	578.4027 (100%)					416.3502, 398.3325, 98.0952
				70 V	98.0962 (100%)	578.4024 (87.88%)	416.3521 (31.34%)	398.3412 (15.84%)	85.0280 (11.21%)	81.0693, 69.0339, 56.0484
	P21	14.36	576.3896	50 V	576.3865 (100%)					414.3328, 396.3207, 98.0976
				70 V	576.3874 (100%)	98.0964 (86.23%)	414.3357 (49.53%)	396.3262 (17.48%)	81.0689 (14.48%)	85.0290, 67.0554, 56.0503, 55.0535
	P38	27.87	414.3365	50 V	98.0964 (100%)	112.1111 (16.07%)	414.3349 (11.91%)			138.1264, 81.0696, 56.0498
				70 V	98.0961 (100%)	56.0500 (38.10%)	81.0704 (19.09%)	55.0545 (16.29%)	79.0537 (11.81%)	138.1269, 112.1106, 91.0538, 67.0538
Jervine type	**P12**	12.52	428.3159	50 V	67.0544 (100%)	114.0905 (69.88%)	84.0804 (51.99%)	109.1008 (43.79%)	81.0700 (41.04%)	412.3201, 410.2883, 351.2410, 107.0850, 105.0696, 95.0858, 93.0699, 85.0656, 79.0540, 57.0704, 55.0542
				70 V	67.0543 (100%)	79.0539 (30.53%)	84.0808 (29.32%)	55.0544 (27.75%)	81.0704 (27.55%)	142.0751, 114.0920, 109.1010, 105.0695, 95.0861, 93.0713, 91.0547, 57.0711
Veratramine type	**P2**	5.83	476.3375	50 V	128.1062 (100%)	458.3220 (12.62%)	98.0962 (10.91%)			440.3116, 422.3076, 410.2646, 366.2439, 164.1452, 138.1268, 124.1123, 116.1073, 110.0954, 85.0643, 69.0345, 55.0536
				70 V	128.1062 (100%)	124.1115 (27.18%)	98.0967 (24.35%)	110.0965 (23.76%)	86.0608 (18.91%)	268.2112, 228.1732, 202.1570, 164.1443, 138.1267, 79.0552, 69.0337, 55.0549
	P5	9.70	460.3426	50 V	128.1063 (100%)	98.0967 (10.39%)				442.3294, 424.3196, 173.0935, 138.1276, 110.0969, 95.0839, 85.0646, 69.0345, 67.0549, 55.0550
				70 V	128.1071 (100%)	67.0549 (31.64%)	98.0972 (29.40%)	86.0600 (29.13%)	95.0854 (28.76%)	394.2652, 138.1285, 155.0827, 145.1007, 138.1285, 124.1121, 110.0956, 91.0545, 55.0550

Table 1 (*Continued*)

Skeleton type	No.	t_R (min)	$[M+H]^+$	CE	Top five ions in abundance ≥10%	Other ions				
	P9	11.22	460.3425	50 V	128.1070 (100%)	98.0968 (10.41%)				442.3222, 424.3214, 422.3035, 392.2555, 311.1984, 112.1118, 105.0695, 95.0848, 86.0607, 85.0652
				70 V	128.1061 (100%)	67.0547 (33.98%)	105.0695 (30.18%)	98.0963 (28.38%)	86.0598 (24.95%)	422.3021, 392.2541, 157.1012, 145.0996, 138.1263, 124.1113, 119.0849, 117.0689, 112.1118, 110.0953, 91.0541, 79.0538, 55.0545
	P14	12.89	442.3309	50 V	124.1119 (100%)	166.1581 (83.06%)	95.0846 (70.19%)	139.1346 (62.94%)	110.0968 (55.77%)	424.3198, 311.2015, 285.1865, 145.1031, 98.0965, 93.0702, 85.0645, 67.0546, 55.0547
				70 V	124.1109 (100%)	91.0542 (64.35%)	67.0542 (60.29%)	79.0546 (53.83%)	105.0687 (43.43%)	181.1034, 166.1592, 136.1109, 110.0958, 98.0970, 55.0541
	P23	16.61	444.3458	50 V	128.1066 (100%)	105.0693 (94.11%)	95.0855 (90.20%)	147.1163 (79.83%)	93.0701 (76.92%)	426.3268, 269.1904, 251.1780, 107.0853, 98.0960, 81.0705, 69.0337, 55.0542
				70 V	105.0698 (100%)	91.0544 (68.59%)	67.0544 (48.79%)	93.0696 (44.92%)	119.0848 (41.61%)	157.1001, 143.0847, 131.0853, 98.0967, 95.0855, 81.0691, 79.0547, 69.0334, 55.0548
	P25	17.48	446.3628	50 V	128.1063 (100%)	107.0855 (54.69%)	145.1011 (47.68%)	105.0700 (33.3%)	95.0854 (33.06%)	428.3488, 253.1946, 81.0703, 67.0551, 55.0547
				70 V	105.0699 (100%)	91.0540 (91.46%)	79.0544 (85.95%)	67.0543 (64.83%)	107.0850 (56.64%)	197.1321, 145.1014, 128.1060, 98.0963, 95.0858, 81.0702, 55.0546
Secosolanidine type	**P33**	25.02	430.3677	50 V	69.0698 (100%)	95.0851 (78.69%)	81.0700 (72.49%)	55.0545 (49.82%)	93.0695 (37.47%)	412.3630, 300.2682, 260.0140, 199.1474, 142.1582, 109.1009, 107.0857, 105.0707, 100.1124, 98.0983, 91.0542, 79.0544, 67.0544
				70 V	55.0548 (100%)	81.0700 (87.21%)	79.0542 (86.23%)	67.0544 (82.97%)	69.0703 (78.37%)	109.1022, 107.0847, 105.0696, 98.0959, 95.0854, 93.0697, 91.0545
	P35	26.57	416.3525	50 V	69.0700 (100%)	81.0702 (94.53%)	95.0851 (86.05%)	55.0545 (66.72%)	67.0541 (39.47%)	398.3487, 135.1147, 131.0854, 121.0997, 109.1016, 107.0856, 105.0696, 93.0703
				70 V	55.0543 (100%)	81.0704 (90.44%)	67.0542 (69.90%)	69.0698 (65.15%)	91.0541 (64.47%)	119.0858, 107.0850, 105.0692, 95.0853, 79.0540
	P41	36.84	428.3521	50 V	69.0697 (100%)	81.0701 (58.67%)	55.0545 (53.27%)	95.0854 (47.58%)	93.0694 (18.18%)	428.3502, 290.0218, 260.0150, 217.1570, 199.1467, 142.1583, 121.1020, 107.0847, 79.0543, 67.0544
				70 V	81.0701 (100%)	55.0545 (98.94%)	67.0544 (66.77%)	69.0703 (59.91%)	79.0546 (50.82%)	142.0752, 109.1025, 107.0855, 105.0705, 95.0853, 93.0700, 91.0542, 77.0387
	P17	13.42	592.4194	50 V	592.4167 (100%)	69.0703 (64.74%)	142.1591 (48.22%)	412.3565 (42.53%)	430.3663 (30.65%)	168.1734, 109.1011, 95.0854, 85.0277, 81.0701, 79.0539, 55.0548
				70 V	69.0699 (100%)	95.0852 (84.64%)	81.0697 (70.97%)	55.0547 (65.64%)	93.0694 (37.98%)	430.3619, 412.3580, 168.1713, 142.1579, 109.1016, 107.0854, 85.0290, 79.0545

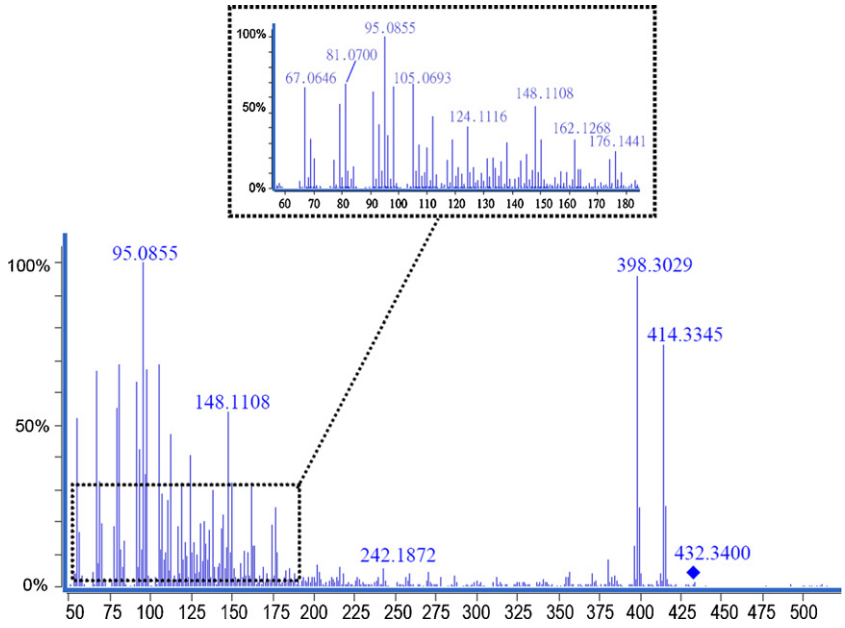

Fig. 3. The ESI$^+$-MS/MS spectra for verticine (**P18**) at 70 V of collision energy.

hydrogen rearrangement and ring cleavage of the basic skeletons through induction effect. The product ion at *m/z* 414.33, with a high abundance, corresponded to the loss of a H_2O molecule (−18 Da), with further peaks appearing at *m/z* 138.12 ($C_9H_{16}N$) and *m/z* 69.07 (C_5H_9) produced by the loss of a $C_{18}H_{28}O_2$ and $C_{22}H_{35}NO_2$, respectively. Another characteristic product ion at *m/z* 112.11 with the elemental composition $C_7H_{14}N^+$, also resulted from hydrogen rearrangement and cleavage of the rings of the basic skeleton, which was also observed in the positive-ion ESI spectra of other FAs. The characteristic product ion at *m/z* 398.30 ($C_{26}H_{40}NO_2$) resulted from successive loss of a CH_4 group and a molecule of H_2O from 432.34. Another major fragment ion at *m/z* 176.14 was formed from $[M+H]^+$ (*m/z* 432.34) by the following sequence: loss of a CH_4, cleavage of the D-ring with the loss of $C_{14}H_{22}O_2$ and then loss of a molecule of H_2O. The fragment ion (*m/z* 176.14) was only observed in ESI-MS/MS spectra of compounds **P18**, **P22**, **P31**. This pathway suggested that the formation of *m/z* 176.14 is concerned with hydroxyl at the 20-position, which could be used as a characteristic ion to characterize this type of alkaloids. Another two protonated positions as we deduced were the hydroxyl group at the N atom in E-ring (Fig. 4B) and the 6-position (Fig. 4C), which forming major fragment ions at *m/z* 81.07 (C_6H_9) and *m/z* 95.08 (C_7H_{11}), respectively. For cevanine type FAs, it is worthy of note that the number of ions exceeding 10% in abundance is no more than three at 50 V CE, and they generally generate $[M+H-H_2O]^+$ or $[M+H]^+$ ions as base peak. While at the CE of 70 V, they generate abundant product ions exceeding 10% in abundance (see Table 1). Therefore, by combination of diagnostic fragment ions and top five ions in abundance ≥10% at different CE, the cevanine type FAs can be distinguished rapidly.

However, there are some exceptional cases of cevanine type FAs that possessing different substituent group or basic skeleton, such as compounds **P13**, **P19** and **P38**. Due to the N → O group, the *N*-oxides **P13** and **P19** are distinct from other cevanine type FAs in the way of decomposition. Instead of strong $[M+H-H_2O]^+$ ion, they produced the base peak ion at *m/z* 112.11 ($C_7H_{14}N$) together with a minor $[M+H-H_2O]^+$ ion and a relatively strong protonated ion $[M+H]^+$. As reported [17], the elimination of OH• radicals generated from the N → O functional group is a characteristic fragmentation pathway of the N-oxides. The formation pathway of base peak ion at *m/z* 112.11 for FAs *N*-oxide **P13** is displayed in Figure S2. Although the compound **P38** is a member of No-C20-OH substituent FAs, it differs with other members in the presence of a double bond between 13 and 17-position of the basic skeleton. As a result, we observed a dominant ion as the base peak at *m/z* 98.09 ($C_6H_{12}N$) instead of $[M+H]^+$ ion at *m/z* 414.33. And the formation of the base peak ion at *m/z* 98.09 was elucidated in Figure S3.

3.2.2. *Jervine type FAs*

The jervine type FAs are hexacyclic compounds that have the furan ring (E) fused onto a piperidine ring system forming an ether bridge between carbon atoms C17 and C23 (see Fig. 1, **P12**). The representative jervine type FAs, peimisine (**P12**), was selected to analyze its fragmentation behavior in QTOF-MS/MS, and the MS/MS data for peimisine are given in Table 1. At both of 50 V and 70 V (CE), the protonated molecule at *m/z* 428.31 gave an ion at *m/z* 67.05 as the base peak by cleavage of the rings of the basic skeleton, with several characteristic product ions at *m/z* 114.09, 84.08, 57.07, 81.07, 410.28 and 55.05. The product ion at *m/z* 114.09 ($C_6H_{12}NO$) was formed by cleavage of the E-ring with the loss of $C_{21}H_{30}O_2$, which owing to the presence of an O bridge between 17, 23-position with its electronic induction effect. Another major fragment ion at *m/z* 84.08 ($C_5H_{10}N$) was produced by protonation at N atom then result in cleavage of rings (E and F) through successive or simultaneous induction and hydrogen rearrangement effects. The characteristic fragment ion at *m/z* 57.07 (C_4H_9) was formed in the similar way as *m/z* 84.08. Due to the presence of the double bond between 12, 13-position, the ionization on pibond was an availability that resulted in the major fragment ion at *m/z* 81.07 (C_6H_9). A minor fragment ion at *m/z* 410.28 ($C_{27}H_{40}NO_2$) was produced by the neutral loss of H_2O, corresponding to the hydroxyl group at 3-position, which was further fragmentized and formed the fragment ion *m/z* at 55.05. Importantly, the fragment ion at *m/z* 55.05, with the elemental composition C_4H_7, was observed with relatively high intensity, which also corroborates our hypothesis that this fragment was produced by cleavage of the rings of the basic skeleton. The fragmentation pathway of reference compound peimisine is shown in Figure S4. It should be noting that we have only one reference compound (peimisine), thus the fragmentation information of jervine type FAs is for reference merely.

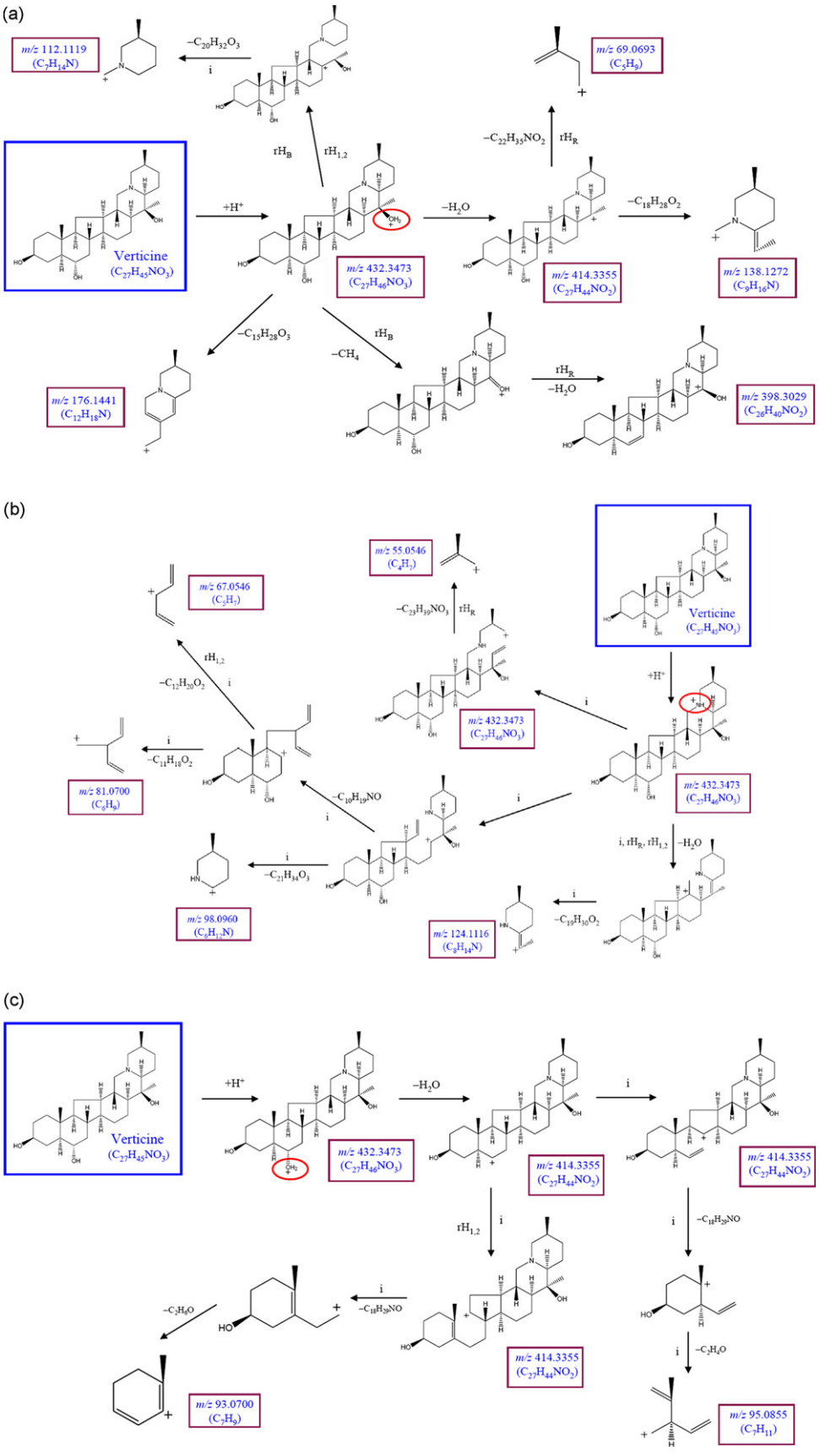

Fig. 4. (A) The proposed fragmentation pathways of verticine (**P18**, cevanine type FAs) with the adding position of H^+ ion at C-20OH. (B) The proposed fragmentation pathways of verticine (**P18**, cevanine type FAs) with the adding position of H^+ ion at N-atom. (C) The proposed fragmentation pathways of verticine (**P18**, cevanine type FAs) with the adding position of H^+ ion at C-6OH.

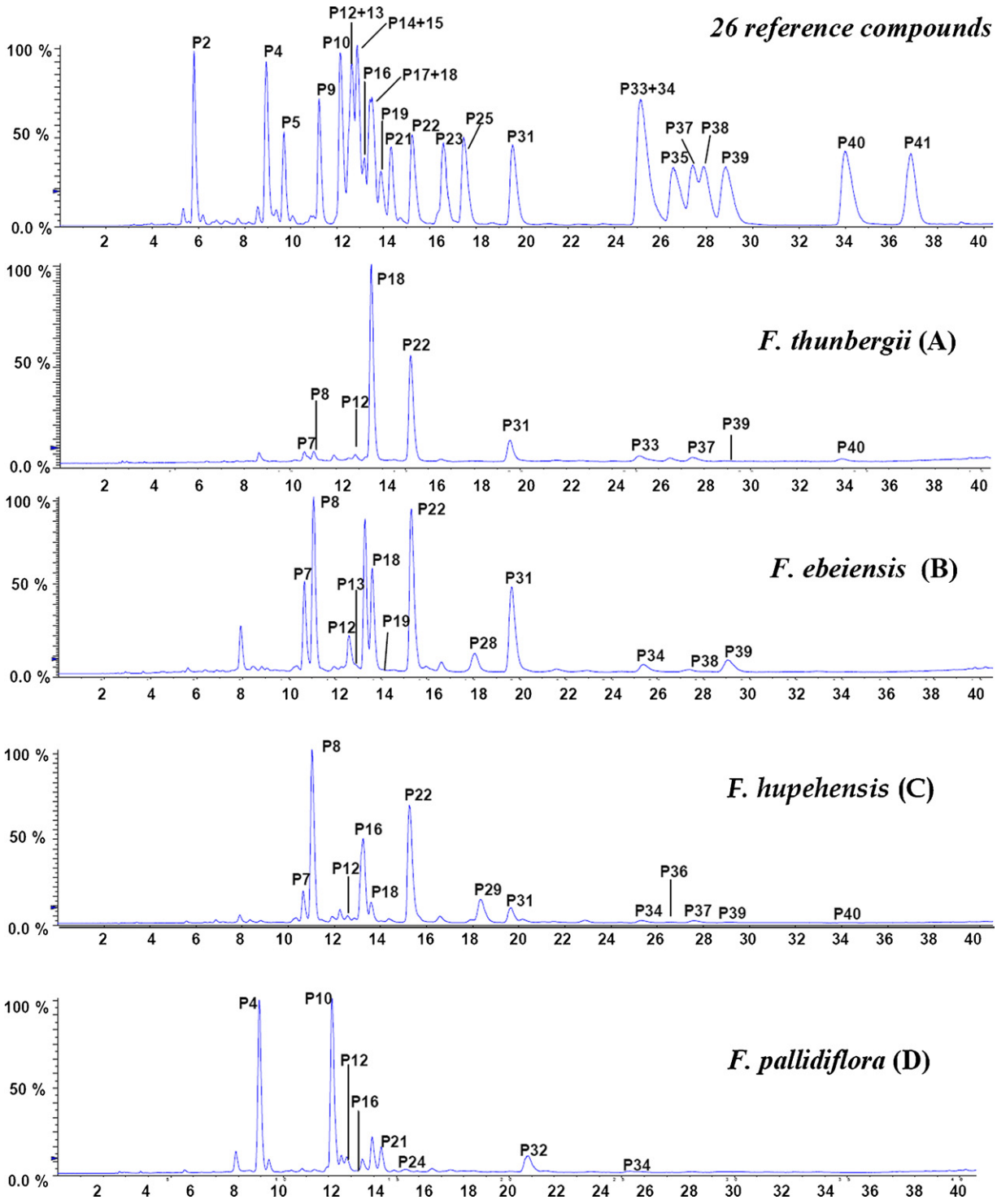

Fig. 5. LC/QTOF-MS total ion chromatograms of the standards and extracts of eight *Fritillaria* species. Chromatographic conditions are described in Section 2.3.

3.2.3. Veratramine type FAs

The typical veratramine type is characterized by the absence of ring E and the presence of an aromatic ring D, although many analogues with an unaromatised ring D are also placed in this group (**P2**, **P5**, **P9**, **P14**, **P23**, and **P25**). Compounds **P2**, **P5** and **P9** yielded an identical dominant ion at *m*/*z* 128.10 ($C_7H_{14}NO$) as the base peak and other minor fragment ions in positive mode with CE of either 50 V or 70 V. The $[M+H-H_2O]^+$ and $[M+H-2H_2O]^+$ ions, with low abundance, can also be observed in ESI-MS/MS spectra, and $[M+H-3H_2O]^+$ ion was rarely shown. As for compounds **P23** and **P25**, they produced the identical base peak at *m*/*z* 128.10 with the CE of 50 V, whereas, it was 105.06 while the CE increase to 70 V. Exceptionally, compound **P14** yielded a strong ion at *m*/*z* 124.11 as the base peak at both CE of 50 V and 70 V, and we explained the formation of this base peak ion in Figure S5. Subsequently, we selected the compound **P2** as the example to elucidate the characteristic fragmentation pathways of veratramine type FAs which was shown in Figure S6.

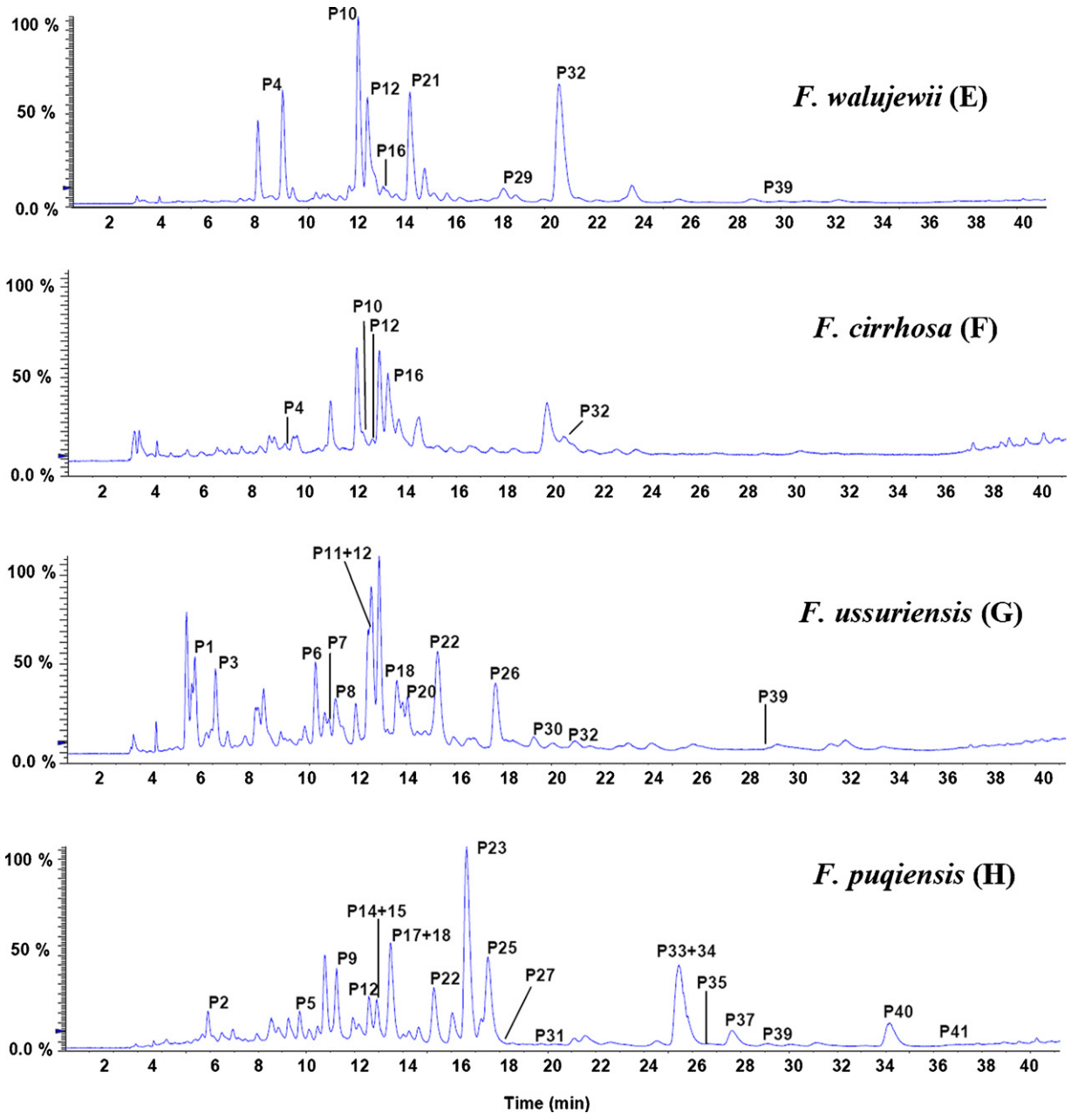

Fig. 5. (*Continued*).

The MS/MS data for compound **P2** are given in Table 1. In positive ion mode with the CE of 70 V, it produced several characteristic fragment ions, such as *m*/*z* 128.10 ($C_7H_{14}NO$), 98.09 ($C_6H_{12}N$), 110.09 ($C_7H_{12}N$) and 86.06 (C_4H_8NO). According to our deduction, the F-ring was shed off to become the base peak ion at *m*/*z* 128.10 ($C_7H_{14}NO$), with further peaks appearing at *m*/*z* 110.09 ($C_7H_{12}N$) and *m*/*z* 86.06 (C_4H_8NO) produced by the neutral loss of a H_2O and C_3H_6, respectively. The fragment ion at *m*/*z* 98.09, with the elemental composition $C_6H_{12}N$, was also observed with relatively high intensity, which resulted from cleavage of the F-ring of the basic skeleton with the loss of a fragment $C_{22}H_{34}O_5$. Another characteristic fragment ion at *m*/*z* 422.30 ($C_{28}H_{40}NO_2$), with low abundance, was formed by successive or simultaneous loss of three molecules of H_2O from the protonated molecule ($C_{28}H_{45}NO_5$). As described above, veratramine type FAs, compared with cevanine type FAs, are more likely to fragmentize. Of particular note is the presence of base peak at *m*/*z* 128.10, which is the characteristic ion of veratramine type FAs.

3.2.4. Secosolanidine type FAs

The secosolanidine type is derived from epiminocholestanes with the amino group incorporated into a piperidine ring, resulting in a pentacyclic carbon framework. Herein, the secosolanidine type FAs investigated consists of compounds **P17**, **P33**, **P35** and **P41**. Likewise, this type FAs are easy to fragmentize. In positive ion mode, they yielded rich characteristic fragmentations at CE of 50 V and 70 V. At the CE of 50 V, compounds **P33**, **P35** and **P41** generated an identical dominant ion at *m*/*z* 69.06 (C_5H_9) as the base peak. With the CE increased to 70 V, the base peak ion of compounds **P33** and **P35** changed into *m*/*z* 55.05 (C_4H_7), and *m*/*z* 81.07 for compound **P41**. Due to the presence of hydroxy group for the compounds **P33** and **P35**, we can observed $[M+H-H_2O]^+$ ion, but not for compound

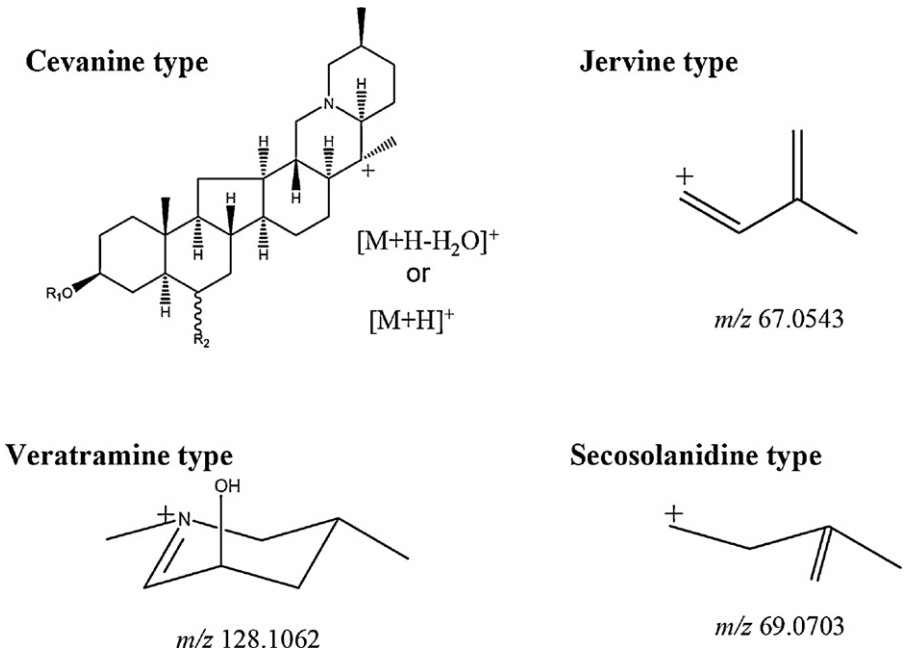

Fig. 6. The structures of key diagnostic fragmentation ions for the different types of FAs.

P41. Compound **P17**, as a gluco alkaloid, produced the characteristic fragment ion at *m*/*z* 85.02 of glucose. Owing to the stability of gluco alkaloid, it yielded protonated ion $[M+H]^+$ at *m*/*z* 592.41 as the base peak at CE of 50 V. With the CE increased to 70 V, it produced similar fragment ions with its aglycon compound **P33** except for neutral loss of a glucose unit (162 Da) generated the aglycone ion $[M+H–Glc]^+$ at *m*/*z* 430.36 ($C_{28}H_{47}NO_2$).

The fragmentation pathway of the secosolanidine type FAs, taking puqietinone (compound **P33**) as an example, was shown in Figure S7. For puqietinone (compound **P33**), it yielded several characteristic product ions at *m*/*z* 55.05, 69.07, 81.07, 67.05, 95.08 and 93.06 at 70 V CE. The base peak at *m*/*z* 55.05 was formed by successive loss of a molecule of water and a neutral fragment of $C_{24}H_{39}NO$ from the protonated ion by cleavage of A-ring. Another dominant ion at *m*/*z* 69.07 resulted from cleavage of piperidine ring of the base skeleton. The product ion at *m*/*z* 67.05, formed by cleavage of B-ring, as well as the product ion at *m*/*z* 95.08 and 93.06, indicated that the protonate position is the carbonyl of B-ring. In addition, the fragment ion at *m*/*z* 81.07, with the elemental composition C_6H_9, was also observed with relatively high intensity, which corroborates our hypothesis that this fragment was produced by cleavage of the rings of the basic skeleton. Notably, the presence of peak at *m*/*z* 69.07 with high abundance could be used as a character to characterize this type of FAs.

3.3. On-line characterization of FAs from extracts of eight *Fritillaria* species

LC/QTOF-MS experiments were carried out to analyze the components in extracts of eight *Fritillaria* species. The total ion chromatograms of the extracts are shown in Fig. 5(A–H). From the LC/QTOF-MS profiles of the eight *Fritillaria* species, 41 FAs were found and characterized in positive-ion mode. The salient information is shown in Table S1, where peaks **P2**, **P4**, **P5**, **P9**–**10**, **P12**–**19**, **P21**–**23**, **P25**, **P31**, **P33**–**35** and **P37**–**41** could be unambiguously assigned to the reference compounds, respectively, by comparison of the retention times (t_R) and MS/MS data with those of the standard FAs. The other 15 peaks were tentatively identified, as discussed below.

Peak 1 (**P1**) gave a minor protonated molecule at *m*/*z* 464.33 with the formula $C_{27}H_{46}NO_5$ in positive ion mode, which yielded $[M+H-H_2O]^+$ ion as base peak at either 50 V or 70 V CE and with only two ions exceeding 10% in abundance at 50 V CE. Meanwhile, $[M+H-3H_2O]^+$ ion could be observed with low abundance, which indicates that **P1** possesses at least three hydroxy groups. The above information drops a hint that **P1** is a member of C20-OH substituent cevanine type FAs. Due to the fact that **P1** could be only detected in *F. ussuriensis*, according to a previous report [26], it was assigned to pingpeimine A. Similarly, peak 3 (**P3**), with the $[M+H]^+$ formula $C_{27}H_{44}NO_6$, was tentatively identified as pingpeimine C [27]. By accurate mass measurements for molecular ion, peak 6 (**P6**) gives the formula $C_{27}H_{37}NO_3$ (the index of hydrogen deficiency is 10), which indicates that there must be some unsaturated bonds in its multiple-ring basic skeleton. **P6**, only found in *F. ussuriensis*, yielded a predominant $[M+H-H_2O]^+$ in positive ion mode with only two ions exceeding 10% in abundance at 50 V, which suggests that **P6** is also a cevanine type FA. Through analyzing and combining previous report [28], **P6** was tentatively identified as ussuriedine. For the **P26**, the MS/MS spectra revealed the protonated molecule ion peak ($[M+H]^+$) at *m*/*z* 416.31 and the base peak at *m*/*z* 164.14. The molecular formula of **P26** ($C_{26}H_{41}N0_3$), obtained by accurate mass measurement for molecular ion, was one carbon less than those of known C-nor D-homo steroidal alkaloids, which was in accordance with pingbeinone that has been reported in the previous literature [29]. Thus, **P26** was tentatively identified as pingbeinone.

The **P30** in the *F. ussuriensis* extract has an MW of 409.3 Da, which was confirmed by the $[M+H]^+$ ion at *m*/*z* 410.30 with the formula $C_{27}H_{40}NO_2$. It yielded $[M+H]^+$ ion as the base peak with only two ions exceeding 10% in abundance at 50 V CE, which suggests that **P30** is a member of No-C20-OH substituent cevanine type FAs. Heilonine, a cevanine type FAs with MW 409.3 Da, has been reported to be present in *F. ussuriensis* [29], and its formula $C_{27}H_{39}NO_2$ with 9 units of unsaturation was in accordance with that of compound **P30**. Thus, **P30** was considered as being due to heilonine. By the same way, **P29**, **P32** and **P36** were tentatively identified as hupehenine [30], sinpeinine A [31] and hupehenirine [30], respectively.

Several cevanine type gluco alkaloids, **P7**, **P8**, **P20**, **P24**, **P27** and **P28**, were observed in herbal extracts. For **P7**, observed in plant samples **A**–**C**, it gave a minor protonated molecule at *m*/*z* 594.39 with the formula $C_{33}H_{56}NO_8$ in positive ion mode, which yielded $[M+H-H_2O]^+$ ion as base peak at either 50 V or 70 V CE and with only two ions exceeding 10% in abundance at 50 V CE. Moreover, it produced a relative high-abundance $[M+H-Glc]^+$ ion and a characteristic fragment ion at *m*/*z* 85.02 of glucose, which indicates that **P7** is a gluco alkaloid. Combining the above informations and literatures [32], we draw a conclusion that **P7** was assigned to zhebeininoside. Similarly, **P8**, **P20**, **P24**, **P27** and **P28**, were tentatively identified as zhebeinone-3-*β*-D-glucoside/verticinone-3-*β*-D-glucoside, pingbeinone-3-*β*-D-glucoside [33], yibeinoside B [34], yubeiside [35] and ebeiedine-3-*β*-D-glucoside, respectively. Moreover, **P11** gave a protonated molecule at *m*/*z* 608.41 ($C_{34}H_{58}NO_8$) and a minor characteristic fragment ion at *m*/*z* 85.02 due to the presence of glucose, which indicates that **P11** is also a kind of gluco alkaloid. As shown in Table S1, **P11** generated at least five fragment ions exceeding 10% in abundance at 50 V CE, suggested that **P11** does not belong to cevanine type FAs. Due to the fact that **P11** could be only detected in *F. ussuriensis*, according to a previous report [36], it was tentatively identified as pingbeininosine.

4. Conclusions

In this work, the fragmentation patterns of different sub-classes of FAs, including cevanine type, jervine type, veratramine type and secosolanidine type FAs, have been systematically studied by means of ESI QTOF-MS/MS. Based on fragmentations analysis and accurate mass measurements of molecular ions and product ions of 26 reference FAs in positive ion mode, fragmentation pathways have been proposed for the FAs and applied to characterize the FAs in eight medicinal plant extracts. In this paper, we mainly use diagnostic ions and the relative abundances and amounts of major fragment ions to distinguish and identify sub-classes of FAs, such as predominant $[M+H-H_2O]^+$ or $[M+H]^+$ ion with no more than five ions exceeding 10% in abundance at 50 V CE indicating cevanine type FAs, *m*/*z* 128.10 or 124.11 as base peak indicating veratramine type FAs, and *m*/*z* 69.06 as base peak with more than five ions exceeding 10% in abundance indicating secosolanidine type FAs. The structures of key diagnostic fragmentation ions for these types of FAs were given in Fig. 6. It is also worthy of note that some minor fragment ions, such as $[M+H-3H_2O]^+$, $[M+H-Glc]^+$, *m*/*z* 85.02, and *m*/*z* 112.11, can provide structural information of the basic skeleton and its substituents. For example, the presence of $[M+H-3H_2O]^+$ ion indicates that the target compound contains polyhydroxy, while $[M+H-Glc]^+$ and *m*/*z* 85.02 ions indicate the presence of glycon.

Based on the fragmentation patterns of the reference compounds, a total of 41 major FAs were screened and identified in eight *Fritillaria* species by the LC/QTOF-MS/MS method, including 29 cevanine type FAs, 1 jervine type FAs, 6 veratramine type FAs and 5 secosolanidine type FAs. The results of this study clearly demonstrated the potential of ESI QTOF-MS/MS for the rapid and sensitive structural elucidation of the multi-groups of constituents in *Fritillaria* species, and open perspectives for similar studies on other medicinal herbs and preparations. It can be foreseen that the combined use of HPLC and QTOF-MS/MS will be an impressive tool for separating, characterizing and predicting components in complex natural matrices.

Acknowledgments

The authors greatly appreciate financial support from the National Science and Technology Major Project 'Creation of Major New Drugs' from China (No. 2009ZX09502-020), Program for Changjiang Scholars and Innovative Research Team in University (No. IRT0868) and Program for New Century Excellent Talents in University (NCET-07-0850) awarded to Hui-Jun Li.

Appendix A. Supplementary data

Supplementary data associated with this article can be found, in the online version, at doi:10.1016/j.chroma.2010.09.019.

References

[1] I. Sho, K. Michiharu, N. Tetsuo, Chem. Pharm. Bull. 11 (1963) 1337.
[2] K. Kaneko, M. Tanaks, U. Nakaoka, Y. Tanaka, N. Yoshida, H. Mitsuhshi, Phytochemistry 20 (1981) 327.
[3] G. Lin, P. Li, S.L. Li, S.W. Chan, J. Chromatogr. A 935 (2001) 321.
[4] Z.J. Shang, X.L. Liu, Chin. J. Med. Hist. 25 (1995) 38.
[5] K. Kaneko, T. Katsuhara, H. Mitsuhashi, Tetrahedron Lett. 27 (1986) 2387.
[6] H. Oh, D.G. Kang, S.Y. Lee, Y.M. Li, H.S. Lee, Planta Med. 69 (2003) 564.
[7] Atta-ur-Rahman, M.N. Akhtar, M.I. Choudhary, Y. Tsuda, B. Sener, A. Khalid, M. Parvez, Chem. Pharm. Bull. 50 (2002) 1013.
[8] Atta-ur-Rahman, A. Farooq, M.I. Choudhary, A.H. Gilani, F. Shaheen, R.A. Ali, F. Noor-e-ain, B. Sener, Planta Med. 60 (1994) 377.
[9] A.H. Gilani, F. Shaheen, A. Christopoulos, F. Mitchelson, Life Sci. 60 (1997) 535.
[10] Y. Jiang, H.J. Li, P. Li, Z.H. Cai, W.C. Ye, J. Nat. Prod. 68 (2005) 264.
[11] Y.H. Zhang, H.L. Ruan, H.F. Pi, J.Y. Cai, F.B. Zeng, W. Zhao, J.Z. Wu, Chin. Tradit. Herb. Drugs 36 (2005) 1205.
[12] H.J. Li, Y. Jiang, P. Li, Nat. Prod. Rep. 23 (2006) 735.
[13] J.L. Zhou, P. Li, H.J. Li, Y. Jiang, M.T. Ren, Y. Liu, J. Chromatogr. A 1177 (2008) 126.
[14] L.W. Qi, X.J. Gu, P. Li, Y. Liang, H.P. Hao, G.J. Wang, Rapid Commun. Mass Spectrom. 23 (2009) 2151.
[15] Z.Y. Zhu, H. Zhang, L. Zhao, X. Dong, X. Li, Y.F. Chai, G.Q. Zhang, Rapid Commun. Mass Spectrom. 21 (2007) 1855.
[16] H.L. Li, J. Tang, R.H. Liu, M. Lin, B. Wang, Y.F. Lv, H.Q. Huang, C. Zhang, W.D. Zhang, Rapid Commun. Mass Spectrom. 21 (2007) 869.
[17] X.S. Miao, R.E. March, C.D. Metcalfe, Int. J. Mass Spectrom. 230 (2003) 123.
[18] C.M. Li, X.L. Zhang, X.Y. Xue, F.F. Zhang, Q. Xu, X.M. Liang, Rapid Commun. Mass Spectrom. 22 (2008) 1941.
[19] Y. Zhou, Q.B. Han, J.Z. Song, C.F. Qiao, H.X. Xu, J. Chromatogr. A 1206 (2008) 131.
[20] G. Lin, Y.P. Ho, P. Li, X.G. Li, J. Nat. Prod. 58 (1995) 1662.
[21] H.J. Li, Y. Jiang, P. Li, W.C. Ye, Chem. Pharm. Bull. 54 (2006) 722.
[22] Y. Jiang, P. Li, H.J. Li, H. Yu, Steroids 71 (2006) 843.
[23] P. Lee, Y. Kitamura, K. Kaneko, M. Shiro, G.J. Xu, Y.P. Chen, H.Y. Hsu, Chem. Pharm. Bull. 36 (1988) 4316.
[24] P. Li, Y. Kitamura, K. Kaneko, M. Shiro, G.J. Xu, Y.P. Chen, H.Y. Hsu, Phytochemistry 31 (1992) 2190.
[25] B. Kasprzyk-Hordem, R.M. Dinsdale, A.J. Guwy, J. Chromatogr. A 1161 (2007) 132.
[26] D.M. Xu, B. Zhang, H.R. Li, M.L. Xu, Acta Pharm. Sin. 17 (1982) 355.
[27] D.M. Xu, C.H. He, S.Q. Wang, E.X. Huang, M.L. Xu, X.G. Wen, Acta Pharm. Sin. 25 (1990) 127.
[28] K. Yukie, N. Makoto, K. Koh, Tetrahedron 45 (1989) 5755.
[29] K. Yukie, N. Makoto, K. Koh, Tetrahedron 45 (1989) 7281.
[30] H.L. Ruan, Y.H. Zhang, J.Z. Wu, Nat. Prod. Res. Dev. 14 (2001) 80.
[31] D.M. Xu, S. Arihara, N. Shoji, X.W. Yang, E.X. Huang, C.S. Li, Acta Pharm. Sin. 25 (1990) 795.
[32] J.X. Zhang, A.N. Lao, R.S. Xu, Acta Bot. Sin. 35 (1993) 238.
[33] D.M. Xu, B. Zhang, Y.W. Xiao, Acta Pharm. Sin. 18 (1983) 868.
[34] Y.J. Xu, D.M. Xu, D.B. Cui, E.X. Huang, X.Q. Jin, S.Y. Lin, M.M. Yan, Acta Pharm. Sin. 28 (1993) 192.
[35] J.X. Zhang, A.N. Lao, R.S. Xu, Acta Bot. Sin. 35 (1993) 963.
[36] D.M. Xu, M.L. Xu, S.Q. Wang, E.X. Huang, X.G. Wen, J. Nat. Prod. 53 (1990) 549.